JOURNAL OF PROPULSION AND POWER
Vol. 14, No. 6, November–December 1998

Microwave Plume Measurements of a Closed Drift Hall Thruster

Shawn Ohler,* Brian E. Gilchrist,† and Alec Gallimore‡
University of Michigan, Ann Arbor, Michigan 48109-2118

The plasma plume from a closed drift hall thruster has been characterized using a 17-GHz microwave diagnostic system. Electron number density profiles are obtained throughout the thruster plume via differential phase measurements. A functional model of plasma density has been developed combining a near-field Gaussian beam term and a far-field point source expansion term. An outcome of this work is a mapping of the transition region between the near- and far-field plume. An indication of slight plume asymmetry is obtained by evaluating total integrated density measurements along rays emanating from the thruster. Additional evaluations have determined the plasma plume effect on attenuation and spectral characteristics of a wave transmitted through the plume. The attenuation was small, with slightly over 2 dB loss at 0.09 m along the thruster axis. However, ray-tracing attenuation modeling based on plasma density profiles indicates a greater effect for lower-frequency operation. The spectral data of the signal transmitted through the plume exhibited clear 26-kHz harmonic sidebands and added broadband noise. Estimates of potential impact to communication and other electromagnetic satellite systems can be obtained directly from the measurements and from the electron number density distribution models derived from the measurements.

Nomenclature

c = speed of light, m/s
e = electron charge, C
$FN(x)$ = Gaussian distribution function of the antennas
f = frequency, Hz
m_e = electron mass, kg
n_c = $(f/8.98)^2$, critical or cutoff density, m^{-3}
$n(r)$ = local electron density in the plume, m^{-3}
q = spatial frequency, m^{-1}
R = maximum radial extent of the plume for Abel analysis, m
r = radial position from thruster, m
x = spatial position along measurement axis, m
ε_0 = permittivity of free space, F/m
θ = angle from thruster axis, rad
λ_i = wavelength, m
ρ = radial position from thruster axis, m
ϕ = phase angle, rad
ω = radial frequency, rad

I. Introduction

CLOSED drift electric propulsion is currently being tested and considered for use aboard next-generation spacecraft for North–South stationkeeping, repositioning, and orbit transfer. Closed drift thrusters (CDTs) are attractive in these roles because of their high thruster efficiency and specific impulse (I_{sp}) of 1300–2700 s, optimal for many of these missions.[1] Understanding possible plume effects on electromagnetic signals is important for evaluating spacecraft integration issues. Using a large vacuum facility with proper placement of antennas, it is possible to characterize directly the plasma effects on electromagnetic signal phase, amplitude, and spectral content. These same measurements can also be used to measure plume plasma density nonintrusively, where data can be used as the basis for predictive models of effects on electromagnetic signals at various frequencies.[2]

Previous CDT studies have reported on various aspects of their operation and spacecraft integration.[2–8] However, only limited measurements of plume impact on electromagnetic signals have been given.[2,7] A number of studies have reported on plume parameters at limited locations such as electron number density, electron temperature, ion velocity, and ion energy.[1,8–11]

Characterization of the plume through microwave diagnostics provides a nonintrusive method to accurately characterize the plasma. The use of microwaves avoids local perturbations of the flow and probe heating inherent in intrusive diagnostics close to the thruster. In addition, a microwave diagnostic system provides a direct measure of communication issues such as power loss and noise increase.

Here, we report on differential phase mapping measurements that lead to the determination of electron number density. Also reported are power spectral density results that will expand on previous spectral measurements at lower frequencies. Finally, direct measurement of attenuation will provide the first reported direct experimental indication of power loss.

The following section reviews the theory of microwave interferometry, the Abel inversion technique as applied to our situation, and the experimental apparatus including the thrusters, vacuum chamber, and positioning system in addition to the microwave measurement system. In Sec. III, experimental results are presented. Section IV reports on a functional model of the plume plasma density. Plume asymmetry is estimated, and measurement accuracy of the experimental system is assessed. Finally, Sec. V contains a summary of results and accomplishments.

II. Experimental System and Theory of Operation

All experiments reported were performed at the Plasmadynamics and Electric Propulsion Laboratory (PEPL) at the University of Michigan in a 9-m-long by 6-m-diam stainless-steel vacuum chamber. The facility is evacuated by six 0.81-m-diam

Presented as Paper 95-2931 at the AIAA/ASME/SAE/ASEE 31st Joint Propulsion Conference, San Diego, CA, July 10–12, 1995; received Feb. 17, 1996; revision received Aug. 20, 1997; accepted for publication June 17, 1998.

*Research Assistant, Electrical Engineering. Member AIAA.
†Associate Professor, Electrical Engineering and Space Science, 1301 Beal Avenue. Member AIAA.
†Assistant Professor, Aerospace Engineering, 1320 Beal Avenue. Member AIAA.

diffusion pumps, each rated at 32,000 l/s on nitrogen (with water-cooled cold traps), backed by two 2000-cfm blowers, and four 400-cfm mechanical pumps. These pumps give the facility a measured overall pumping speed for xenon of over 27,000 l/s. Plume diagnostics are performed through the use of a probe positioning system. The table contains two rotary platforms on a linear stage with 1.5 m of travel in the radial direction on a 0.9 m travel axial stage. The entire probe positioning system is mounted on a movable platform to allow for measurements to be made throughout the chamber. A more complete description of the experimental facilities can be found in Marrese et al.[11]

A diagram of the Hall thruster is shown in Fig. 1. It is a commercial-grade model SPT-100 built by the Russian Fakel Enterprises and on loan from Space System/Loral, and previously tested by the NASA Lewis Research Center[1,4,8–10] and the Jet Propulsion Laboratory.[5] The i.d. of the outer ceramic ring is 0.1 m and the cathodes are LaB_6 thermionic emitters. A more complete description of the thruster can be found in Refs. 4 and 5.

The microwave system (Fig. 2) used for these measurements has been designed to work in the Ku band (12–18 GHz).[12–14] Density measurements are taken using a 17-GHz signal transmitted through the plume of the thruster orthogonally to the thruster axis at a transmitted power of less than 0.1 mW. The measurement system consists of a computer-controlled network analyzer connected to a microwave frequency conversion (both up converting and down converting) and amplification circuit and two lens-corrected horn antennas each with 7- to 8-deg beam widths. The antenna beam patterns are described by a Gaussian distribution function with a standard deviation of 0.024 m.[14] The positioning table moves the microwave system throughout the plume at a rate of 0.01 m/s. Measurement noise is a result of small vibrations of the measurement system while moving and the 20-dB power difference between the transmitted and received microwave signal. The total resulting phase noise is ±2 deg and the amplitude noise is ±0.2 dB. The stability of the microwave system enables a straightforward differential comparison of attenuation and phase with and without the plasma present.

The measurement system provides three data. Differential phase and differential amplitude are obtained through the network analyzer transmission coefficients. The power spectral density is attained through using the network analyzer's transmitted signal and by recording the frequency spectrum on a spectrum analyzer from the received signal.

All of the measurements provide information concerning electromagnetic system impact. The phase shift measurements provide additional information related to the line-integrated

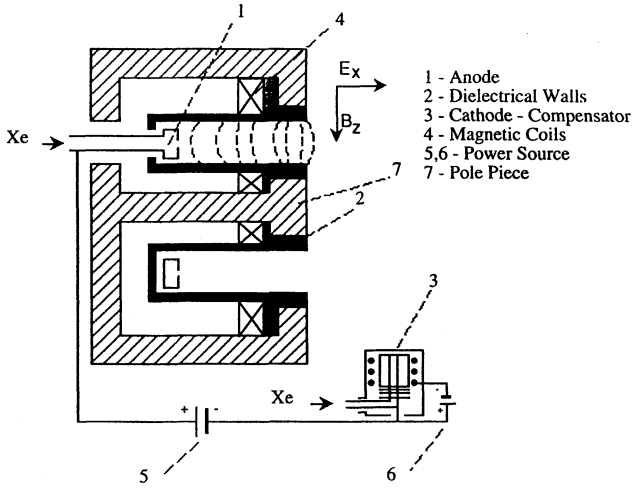

Fig. 1 Diagram of SPT-100 with discharge chamber pointed upward.

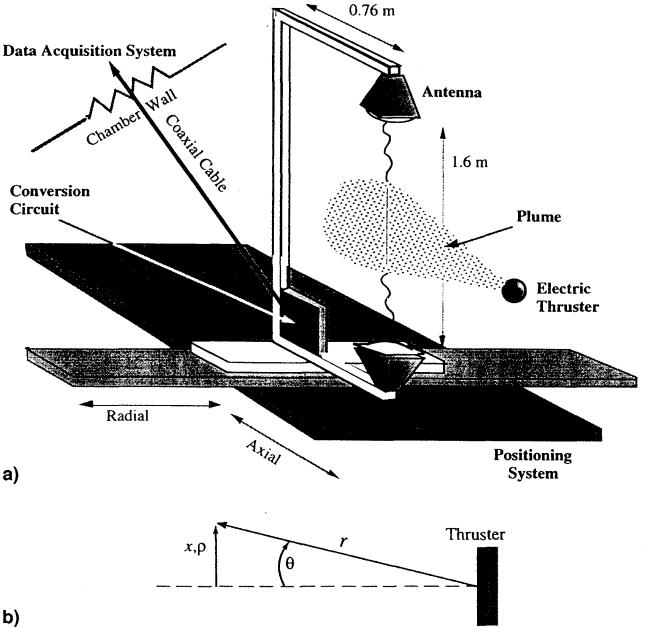

Fig. 2 a) Microwave system schematic and b) diagram of coordinate systems for the microwave system and thruster that is used in the data analysis. (p is a radial coordinate originating at the thruster axis and x is along the microwave transmission direction).

plasma electron density through microwave interferometric analysis.[14] By making multiple measurements along a plane perpendicular to the thruster axis and assuming radial symmetry, the local electron density can be found using an Abel inversion technique.[15–17]

The chordal phase measurements and their gradient in the measurement plane can be used according to the Abel inversion relation[15] to obtain radial electron density estimates throughout the radial plane. However, noise introduced by the derivative of raw data and the singularity at the integral endpoint can create difficulties in applying the inversion directly. Therefore, several methods have been used in the past to avoid these problems.[14,18] In the analysis used in this study, an implementation of a low-pass filter[19] coupled with a double transform of the Abel integral[20] reduces these computational issues. Specifically, the Abel integral is manipulated into a double transform; first a spatial Fourier transform followed by a Hankel transform:

$$n(\rho) = 2\lambda n_c \int_0^{+\infty} qJ_0(2\pi\rho q) \int_{-\infty}^{+\infty} \phi \exp(-j2\pi xq)\, dx\, dq \quad (1)$$

Also, after performing the Fourier transform, a low-pass filter can easily be implemented in the transform domain. Thus, data noise can be filtered in a straightforward manner with removal of the singularity.

III. Experimental Results

The SPT-100 was nominally operated at 300 V and 4.5 A discharge voltage and current, respectively, using xenon propellant at a flow rate of 5.5 mg/s through the anode and 0.29 mg/s through the hollow cathode. (A single flow control was available with 5% of the total flowing through the cathode.) To maintain the discharge current, the flow was changed by no more than 0.5 mg/s of total flow. The tank pressure was maintained below 6×10^{-3} Pa (5×10^{-5} torr) throughout the experiments.

Measurements of the differential phase, differential amplitude, and power spectral density are presented. The phase measurements provide a direct indication of the electron density,

whereas the amplitude and spectral measurements indicate additional effects of the thruster plume on a microwave signal.

A. Electron Density Measurements

Differential phase measurements have been taken in parallel planes orthogonal to the thruster axis, and measurements were recorded every 0.005 m. The planes are located between 0.09 and 0.90 m axially from the thruster exit plane. Along the axial direction, measurements were taken in 0.03-m increments from 0.09 to 0.39 m and every 0.06 m farther out from the thruster. The spatial resolution along the thruster axis is limited to the sampling resolution. In the orthogonal direction, the measurements are sampled every 0.005 m; therefore, the antenna beam (~0.025 m) is the limit to spatial resolution in this direction. The higher spatial sampling aids in data analysis (however, this is not required for the Abel inversion). The absolute positional uncertainty is approximately ±0.02 m and the relative uncertainty between measurement planes is approximately $\pm 2 \times 10^{-3}$ m.

To determine the local electron number density, the antenna pattern first is removed from the measurements via deconvolution using the calibration distribution function.[14] A digital low-pass boxcar filter then removes the high-frequency noise from the measurement and deconvolution process. The filter cutoff frequency is chosen to minimize high-frequency noise while maintaining the measurement features. The Abel inversion through the transform method then finds the local electron number density in the plume. Finally, for data analysis purposes, the data are transformed from a Cartesian coordinate system into a spherical coordinate system through linear interpolation. Figure 3 shows one set of phase data 0.09 m from the thruster exit plane overlaid with the resulting electron density distribution, which is found through the preceding analysis method.

The results presented here are comparable with the previously reported results within the uncertainty of the measurements. Figure 4 shows electron density measurements at 0.30 m for the microwave measurements and Langmuir probe data taken by Myers and Manzella.[1] The measurements reported here show a peak density of 6.2×10^{16} m^{-3} (±17%) and reduction by a factor of 3 along a similar contour at 21-deg

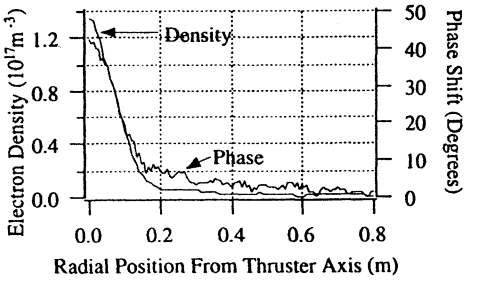

Fig. 3 Overlay of phase measurements and calculated density for the SPT-100 at 0.009 m from thruster exit plane.

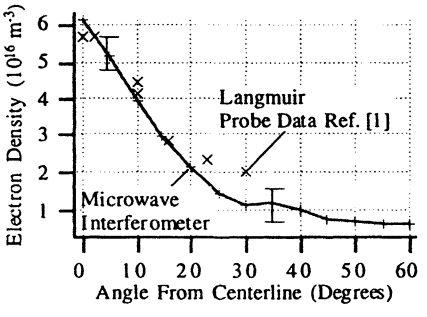

Fig. 4 Comparison of microwave measurements to langmuir probe results taken by Myers and Manzella, 0.3 m from the thruster exit plane.

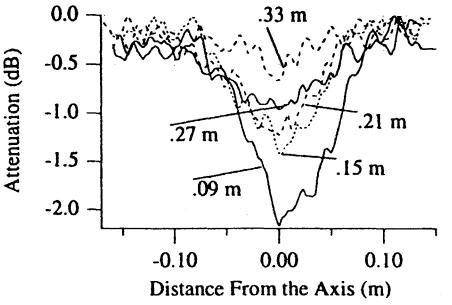

Fig. 5 Attenuation measurements for the SPT-100 showing the trends in five planes orthogonal to the thruster axis.

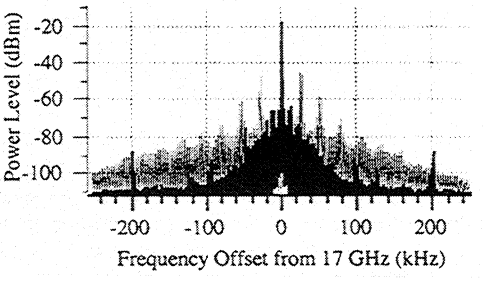

Fig. 6 Power spectral density around the 17-GHz signal for the SPT-100; darker region indicates the baseline noise level.

off centerline. Myers and Manzella report a peak density of 5.7×10^{16} m^{-3} (langmuir probe accurate to ±50%) decreasing by factor of 3 at 22-deg off centerline for the SPT-100 at 0.30 m. The difference in measurements is well within the uncertainty expected of the separate measurements.

B. Attenuation Measurements

Signal power reduction has been explored because high peak density and density gradients exist that can refract on an electromagnetic signal. The SPT-100 plume produces a small degradation in the transmitted signal, which is slightly more than 2 dB of loss at the closest measurement point of 0.09 m. Beyond 0.24 m axially from the thruster and 0.05 m from the thruster axis, the loss is less than 1 dB. Figure 5 presents attenuation measurements for the SPT-100. The minimal reduction in power does not impact the phase measurements, as a greater than 10-dB loss would be required to affect the microwave system resolution.

C. Power Spectral Density

The phase noise produced by the microwave system and the positioning system is ±2 deg. It was expected that oscillations in the discharge current (nominally ±50%) and the plasma found previously by Dickens et al.[6] for the SPT-100 thruster may produce significant additional phase noise. Figure 6 shows the power spectral density for transmission through the plume 0.14 m from the exit plane of the SPT-100 compared with the power spectral density without the plasma plume. Measurements of the broadband noise show that the thruster raises the noise power by 5–25 dB (from −110 dBm) for offsets between 10 kHz and 1 MHz from the 17 GHz signal. In addition, coherent peaks in the frequency spectrum occur at 26 kHz harmonic sidebands, with the largest peaks at approximately −30 dB below the carrier.

IV. Analysis of Results

A. Functional Model of Electron Density

We have developed a plume density model based on the density measurement using a combination of two functions that attempt to bridge the near- and far-field distributions. The near-field term treats the distribution as an ideal Gaussian beam,

while the far-field term models the point source expansion of a plume.[21,22] The following expression mathematically summarizes the plume model:

$$n(r) = C1 \cdot \exp\left[-\left(\frac{r \sin\theta}{C2}\right)^2\right] + \frac{C3}{r^2}\exp\left(-\frac{\theta}{C4}\right) \quad (2)$$

The $r \sin\theta$ term in the Gaussian exponential argument accounts for variations in the plane orthogonal to the thruster axis. The coefficients for the expression are obtained through a least-squares minimization of the difference between the data and the model from 0.12 m radially out to 0.70 m, and for angles 0–50 deg with respect to the thruster center line. The coefficients for this expression used for the SPT-100 are as follows: $C1 = 4.7 \times 10^{16}$ m^{-3}, $C2 = 0.073$ m, $C3 = 1.3 \times 10^{15}$ m^{-1}, and $C4 = 1.1$ rad.

Figure 7 shows the close comparison of the model with the density measurements in the region where the coefficients were optimized. The slight variation in the measurements are representative of the typical thruster variation over time. The measurements shown in Fig. 7 were taken over approximately 30 min. In a test where the microwave system was held at a constant position, the phase varied by 3 deg over a 10-min span. This indicates a variation of 7% in line-integrated electron density.

Figure 8 shows the density contour of the model. As would be expected, farther away from the thruster axis, the free expansion term matches the observed distribution. This model is valid within the measurement region from 0.12 to 0.90 m radially and out to at least 70 deg. It is expected that additional factors will need to be considered outside this region. For example, the first term is a constant as a function of r for $\theta = 0$. However, clearly this term must decay at some distance, depending on collisional effects and plasma neutralization.

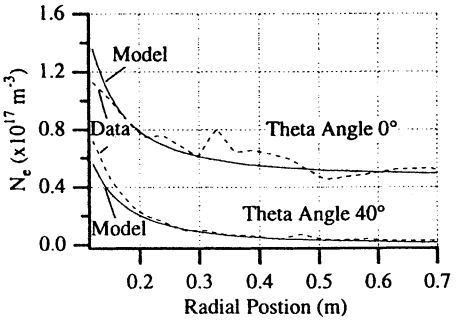

Fig. 7 Electron density of the functional model overlaid on the measured data for constant angles with respect to the SPT-100 centerline.

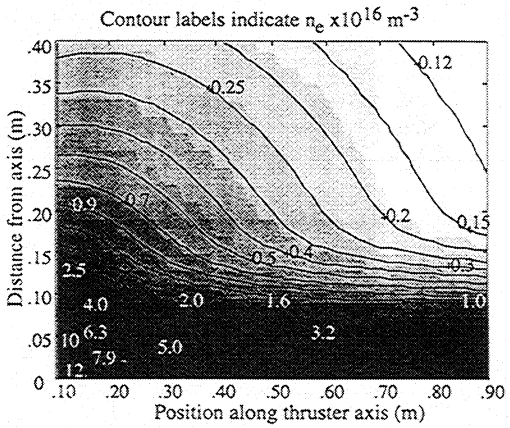

Fig. 8 Electron number density functional model contour plot for the SPT-100.

B. Estimation of Asymmetry

The Abel integral depends on an assumption of radial symmetry; however, the SPT is known to exhibit a small asymmetry.[8] Because only a single cathode is placed to one side of the thruster (see Fig. 1), the primary asymmetry in the SPT thruster configuration is assumed to be caused by the cathode.[8] In the experiments, the cathode is in the horizontal direction and the measurements are in the vertical direction. An estimation of the asymmetry caused by the cathode can be determined through comparison of the phase data from measurements on either side of the thruster axis when the cathode is placed entirely on one side.

The estimation of asymmetry is found by using the phase shift, which measures the line-integrated plasma density along the transmission path. Summing the phase-shift measurements along lines radially outward from the thruster gives an indication of the number of particles in a particular direction. By summing the phase data in the two half-planes with and without the cathode, an asymmetry estimate can be made. The first step is to integrate the number of particles along distinct angular directions. Figure 9 shows the particle flow diagram for the thruster, where the magnitude is a measure of the average number of particles per m per radian along a certain angular direction. By summing the particle number values on either side of the cathode, the off-axis particle vector for the thruster is estimated to be 1.3% of the total or 0.8 deg away from the axis. Manzella[8] reports the thrust vector to be 2% of the total thrust. The thrust vector is an indication of particle flux (not just particle density), but the indication of asymmetry is similar. If all other asymmetry mechanisms produce less variation, then it is expected that the local density error for individual measurement sweeps will be less than 2% of the peak density along the thruster centerline.

C. Comments on Attenuation and Power Spectral Density

While collisional damping sometimes occurs in plasmas, the collision frequency here is expected to be less than 10 MHz and, therefore, much less than the 17-GHz transmission frequency. Thus, the primary cause for attenuation should be refraction effects in the plume. This is verified by applying a two-dimensional ray-tracing algorithm[23,24] that uses the electron density model. Figure 10 shows the calculated ray paths through the plume, and Fig. 11 overlays one of the attenuation sweeps with the ray tracing results. The traces in Fig. 10 are

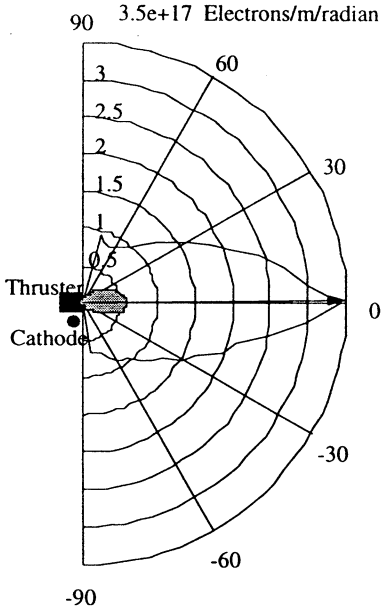

Fig. 9 Integrated particle plot for the SPT-100 showing the number of particles at angles from thruster axis. The total particle vector is only 0.8-deg off axis.

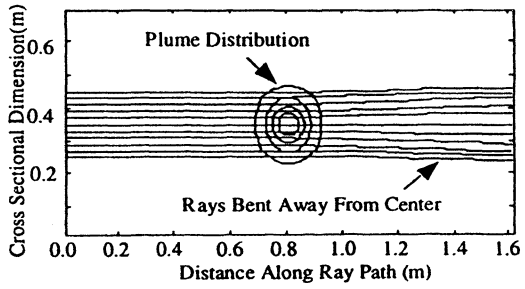

Fig. 10 Ray paths of a 17-GHz signal based on the density model. Parallel ray paths diverge after traversing the plume.

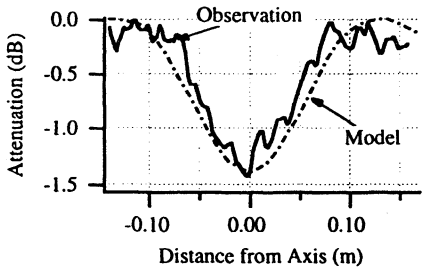

Fig. 11 Overlay of one of the attenuation sweeps and the ray-tracing results, 0.15 m from the exit plane.

0.15 m from the exit plane of the SPT. This not only confirms the expectation that the attenuation is a result of refractive losses, but verifies consistency with our electron density model.

Ray-tracing calculations, 0.15 m from the thruster, were also done at 10 and 6 GHz. The 10-GHz trial has shown a greater than 3.5-dB peak loss, whereas the 6-GHz loss is greater than the 10-dB peak loss. Complete reflection of the signal (infinite attenuation) is achieved at the plasma frequency (2.8 GHz at 0.15 m from the thruster). The refraction of rays is so great that the ray-tracing method is not valid for frequencies below 4.8 GHz at 0.15 m from the thruster. This could have significant impact on lower-frequency microwave signals such as the global positioning system (GPS) that transmits at 1.6 GHz.

The spectral measurements indicated a noise increase between 5 and 20 dB for offsets between 10 kHz and 1 MHz. The added noise power could be of concern for some radar and communications systems. However, the phase differential and amplitude differential measurements made here were not appreciably affected because of the narrow 3-kHz bandwidth of the microwave system. As previously stated, the thruster produced additional phase noise of ± 0.5 deg, which is now attributed to the thruster broadband noise. The added phase noise is filtered along with the measurement system noise.

D. Error Analysis of Density Measurements

The total system measurement error is estimated by examining the individual sources of uncertainty within the measurement and the analysis phases. A basic model of the density based on the phase measurements is used in simulations to assess uncertainty. Each of the factors is varied individually to determine the effect on the final results. The percent difference in the peak electron density for a sweep is used as a figure of merit for the system. Uncertainty in position, phase reference, and filter cutoff in the Abel inversion analysis have all been evaluated by determining how each parameter uncertainty effects the final result. The results are presented for each parameter. The positioning uncertainty results in a peak density variation of $\pm 3\%$. Varying the phase reference produces $\pm 1\%$ density variations. Lastly, uncertainty in the choice of cutoff frequency produces $\pm 10\%$ variation in peak density. This uncertainty dominates because of the semiquantitative nature of choosing the cutoff frequency in comparison with the quantitative nature of the other uncertainties. The 2% error allocated to the effect from asymmetry is also included. An additional 1% is included to account for other uncertainties in the diagnostic system, such as a slight nonideal behavior affecting the plasma model. The total uncertainty is estimated to be $\pm 17\%$. The system has shown a repeatability in the peak density to within 10%, well within the estimated uncertainty.

V. Summary

The electron number density of a closed drift Hall thruster is mapped in vacuum in the region from 0.09 to 0.90 m axially from the thruster, with a discharge voltage of 300 V and a discharge current of 4.5 A. The measurements of the SPT-100 compare well with previous data taken at a constant radial distance of 0.30 m. The peak density in the measurement region 0.09 m axially from the thruster was 1.3×10^{17} m^{-3} for the SPT-100 thruster.

The results were modeled using a functional combination of a Gaussian beam and a point source expansion term in an attempt to bridge the near- and far-field characteristics of the thrusters. The model fits very well in the optimization region from 0.12 to 0.70 m radially from the thruster.

Indications of asymmetry caused by the cathode are derived by summing the particles in the two half-planes, with and without the cathode. These calculations indicate a 0.8-deg off-axis density asymmetry for the SPT-100. The results with the SPT-100 agree with previous measurements using the velocity vector as an indicator of asymmetry. This small asymmetry does not affect the density results beyond the estimated uncertainty.

The spectral measurements indicate a 26-kHz harmonic modulation of the density with broadband noise raising the -110 dBm noise floor between 5 and 20 dB for a spectral range of 10 kHz to 1 MHz. The phase noise indicated by the plasma oscillations produced only a ± 0.5-deg phase variation for our narrow-band system, but could have greater impact on more sensitive radar systems with wider bandwidth and lower operating frequency.

Attenuation measurements showed slightly over 2 dB of loss at the nearest measurement point at 17 GHz. However, the attenuation was measured at below 1 dB, 0.24 m axially from the exit plane and 0.08 m radially out from the thruster centerline. The attenuation produced minimal phase variation. The loss of power is primarily attributed to refraction effects near or within density gradients in the plume. The electron number density functional model has been applied in a ray-tracing algorithm demonstrating consistency with the attenuation measurements. The modeling also indicates that electromagnetic signals operating at lower frequencies, such as GPS, could have significant performance degradation without careful planning of antenna/thruster placement or operational scheduling.

Acknowledgments

This research was funded in part by the U.S. Air Force Office of Scientific Research Grant #F49620-95-1-0331. The Contract Monitor was M. Birkan. The authors would like to thank several students at PEPL, M. Domonokos, J. Foster, J. Haas, S. W. Kim, B. King, and C. Marrese, whose help made the experiments happen. We would also like to thank M. Holladay of the Space Physics Laboratory for his work on coding the ray-tracing model. Our appreciation also goes to V. Liepa and K. Sarabandi for their generous use of equipment. We wish to thank M. Day from Space Systems/Loral for the loan of the SPT-100.

References

[1]Myers, R. M., and Manzella, D. H., "Stationary Plasma Thruster Plume Characteristics," 23rd International Electric Propulsion Conf., Paper 93-096, Sept. 1993.

[2]Ohler, S., Gilchrist, B. E., and Gallimore, A. D., "Microwave Plume Measurements of an SPT-100 Using Xenon and a Laboratory Model SPT Using Krypton," AIAA Paper 95-2931, July 1995.

[3]Pencil, E. J., "Preliminary Far-Field Plume Sputtering of the Stationary Plasma Thruster (SPT-100)," 23rd International Electric Propulsion Conf., Paper 93-098, Sept. 1993.

[4]Sankovic, J., Hamley, J., and Haag, T., "Performance Evaluation of the Russian SPT-100 Thruster at NASA LeRC," 23rd International Electric Propulsion Conf., Paper 93-094, Sept. 1993.

[5]Garner, C. E., Polk, J. E., Goodfellow, K. D., and Brophy, J. R., "Performance Evaluation and Life Testing of the SPT-100," 23rd International Electric Propulsion Conf., Paper 93-091, Sept. 1993.

[6]Dickens, J., Kristiansen, M., and O'Hair, E., "Plume Model of Hall Effect Plasma Thrusters with Temporal Considerations," 24th International Electric Propulsion Conf., Paper 95-171, Sept. 1995.

[7]Dickens, J., Mankowski, J., Kristiansen, M., and O'Hair, E., "Impact of Hall Thrusters on Communication System Phase Noise," AIAA Paper 95-2929, July 1995.

[8]Manzella, D., "Stationary Plasma Thruster Ion Velocity Distribution," AIAA Paper 94-3141, June 1994.

[9]Manzella, D. H., "Stationary Plasma Thruster Plume Emissions," 23rd International Electric Propulsion Conf., Paper 93-097, Sept. 1993.

[10]Absalamov, S. K., Andreev, V. B., Colbert, T., Day, M., Egorov, V. V., Kaufman, M., Kim, V., Korakin, A. I., Kozubsky, K. N., Kudravzev, S. S., Lebedev, U. V., Popov, G. A., and Zhurin, V. V. "Measurement of Plasma Parameters in the Stationary Plasma Thruster (SPT-100) Plume and its Effect on Spacecraft Components," AIAA Paper 92-3156, July 1992.

[11]Marrese, C., Gallimore, A. D., Haas, J., Foster, J., King, B., Kim, S. W., and Khartov, S., "An Investigation of Stationary Plasma Thruster Performance with Krypton Propellant," AIAA Paper 95-2932, July 1995.

[12]Gallimore, A., Reichenbacher, M., and Guiczinski, F., "Near- and Far-Field Plume Studies of a 1kW Arcjet," AIAA Paper 94-3137, June 1994.

[13]Ohler, S. G., Gilchrist, B. E., and Gallimore, A. D., "Non-Intrusive Electron Number Density Measurements in the Plume of a 1 KW Arcjet Using a Modern Microwave Interferometer," *IEEE Transactions on Plasma Science*, Vol. 23, No. 3, 1995, pp. 428–435.

[14]Ohler, S. G., Gilchrist, B. E., and Gallimore, A. D., "Flexible Microwave System to Measure the Electron Number Density and Quantify the Communications Impact of Electric Thruster Plasma Plumes," *Review Scientific Instruments*, Vol. 68, No. 2, 1997, pp. 1189–1194.

[15]Sips, A. C. C., "Reflectometry and Transport in Thermonuclear Plasmas in the Joint European Torus," Ph.D. Dissertation, Eindhoven Univ. Technol., Eindhoven, The Netherlands, 1990.

[16]Wu, H. P., and McCreery, R. L., "Observation of Concentration Profiles at Cylindrical Microelectrodes by a Combination of Spatially Resolved Absorption Spectroscopy and the Abel Inversion," *Analytical Chemistry*, Vol. 61, No. 21, 1989, pp. 2347–2352.

[17]Okada, S., Kiso, Y., Goto, S., and Ishimura, T., "Reduction of the Density Profile of a Field-Reversed Configuration from Detailed Interferometric Measurements," *Journal of Applied Physics*, Vol. 16, No. 12, 1989, pp. 4625–4631.

[18]Lanquart, J. P., "Error Attenuation in Abel Inversion," *J. Comput. Physics.*, Vol. 47, No. 3, 1982, pp. 434–443.

[19]Sharma, S. K., "Density Profile Determination of Cylindrically Symmetric Nonuniform Plasma Spatial Filtering," *Plasma Phys. Contr. Fus.*, Vol. 28, No. 1B, 1986, pp. 391, 392.

[20]Smith, L. M., Keefer, D., and Sudharsnan, S. I., "Abel Inversion Using Transform Techniques," *Journal of Quantitative Spectroscopy & Radiative Transfer*, Vol. 39, No. 5, 1988, pp. 367–373.

[21]Carney, L. M., and Sankovic, J. M., "The Effects of Arcjet Thruster Operating Condition and Constrictor Geometry on the Plasma Plume," AIAA Paper 89-2723, July 1989.

[22]Birkner, G. A., Hallock, H. K., and Ling, H., "Arcjet Plasma Plume Effect on a Microwave Reflector Antenna," *Review of Scientific Instruments*, Vol. 61, No. 10, 1990, 2978–2980.

[23]Ling, H., and Kim, H., "Electromagnetic Scattering from an Inhomogeneous Object by Ray Tracing," *IEEE Transactions on Antennas and Propagation*, Vol. 4, No. 5, 1991, pp. 517–525.

[24]Ling, H., Kim, H., Hallock, G., Birkner, B., and Zamen, A., "Effect of an Arcjet Plume on Satellite Reflector Performance," *IEEE Transactions on Antennas and Propagation*, Vol. 39, No. 9, 1991, pp. 1412–1419.